

# Fabrication of a Blue $M \times N$ Pixel Organic Light-Emitting Diode Video Display Incorporating a Thermally Stable Emitter

Andreas Haldi, Jung B. Kim, Benoit Domercq, Abhishek P. Kulkarni, Stephen Barlow, Angela P. Gifford, Samson A. Jenekhe, Seth R. Marder, and Bernard Kippelen, *Senior Member, IEEE*

**Abstract**—A  $7 \times 11$  pixel blue OLED display was fabricated using a patterned indium–tin–oxide (ITO) substrate. The fabrication process for an  $M \times N$  pixel organic light-emitting diode (OLED) video display including an electrical insulating layer and a physical pixel separator layer is presented. An efficient and thermally stable blue fluorescent organic material, 6,6'-bis((2-*p*-biphenyl)-4-phenylquinoline) (B2PPQ), was used in combination with an evaporated hole-transport small molecule with a high ionization potential.

**Index Terms**—Blue fluorescence, organic light-emitting diodes (OLEDs), passive matrix display.

## I. INTRODUCTION

RECENTLY, organic light-emitting diode (OLED) display technology has advanced sufficiently to enable the mass-production of displays for various applications, such as mobile phones, MP3-players, and televisions [1]. Compared to other display technologies, OLED displays have the advantages of high brightness, wide viewing angle, and low power consumption. However, there is still a need for organic materials with a high thermal stability, with good color purity, and with high photoluminescence quantum yield that can be incorporated into OLED displays.

Manuscript received March 28, 2008; revised June 27, 2008. Current version published March 18, 2009. This work supported in part by the STC Program of the National Science Foundation under Agreement DMR-0120967 and by the Office of Naval Research. This work was performed in part at the Microelectronics Research Center at Georgia Institute of Technology, a member of the National Nanotechnology Infrastructure Network, supported by the National Science Foundation under Grant ECS-03-35765.

A. Haldi, J. B. Kim, B. Domercq, and B. Kippelen are with the School of Electrical and Computer Engineering, and also with the Center for Organic Photonics and Electronics, Georgia Institute of Technology, Atlanta, GA 30332 USA (e-mail: ahaldi@ece.gatech.edu; jungbae.kim@ece.gatech.edu; domercq@ece.gatech.edu; kippelen@ece.gatech.edu).

A. P. Kulkarni is with the Department of Chemical Engineering, University of Washington, Seattle, WA 98195 USA (e-mail: kulkarni@cheme.washington.edu).

A. P. Gifford is with the Department of Chemistry, University of Washington, Seattle, WA 98195 USA (e-mail: gifford@chemistry.washington.edu).

S. Barlow and S. R. Marder are with the School of Chemistry and Biochemistry, and also with the Center for Organic Photonics and Electronics, Georgia Institute of Technology, Atlanta, GA 30332 USA (email: stephen.barlow@chemistry.gatech.edu; seth.marder@chemistry.gatech.edu).

S. A. Jenekhe is with the Department of Chemical Engineering, and also the Department of Chemistry, University of Washington, Seattle, WA 98195 USA (e-mail: jenekhe@cheme.washington.edu).

Color versions of one or more of the figures are available online at <http://ieeexplore.ieee.org>.

Digital Object Identifier 10.1109/JDT.2008.2004782

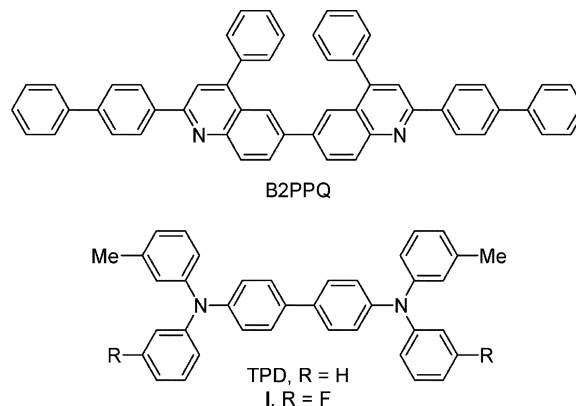


Fig. 1. Molecular structure of the blue fluorescent material B2PPQ and TPD-based small molecules with different substituents.

While high efficiencies and good color purities have been demonstrated for OLED devices with red and green emission, most reports of blue-emitting OLEDs devices show less than 10% external quantum efficiencies [2], [3]. Therefore, a substantial amount of research is currently being done in the synthesis of blue emissive molecules and complexes with high photoluminescence quantum yield and in the fabrication of efficient blue-emitting OLED devices.

Recently, members of our team (S. A. Jenekhe *et al.*) reported on blue fluorescent oligoquinoline derivatives with high glass temperatures. Devices using one of these oligoquinoline derivative, 6,6'-bis((2-*p*-biphenyl)-4-phenylquinoline) (B2PPQ, Fig. 1), as the fluorescent emitter showed deep blue emission with some of the highest efficiencies that can be observed for fluorescent emitters [4]. In these devices, the hole-transport layer, poly(*N*-vinyl-carbazole) (PVK), was spin-coated and the electron-transport and emitting layer of B2PPQ was processed from the vapor phase on top of PVK. However, for the fabrication of displays using shadow masking all layers should preferably be thermally evaporated to ensure uniform film formation on the substrate that is pre-patterned with a separator layer.

In this paper, a detailed process for the fabrication of a blue-emitting  $M \times N$  pixel passive matrix OLED display based on the thermally stable blue fluorescent emitter B2PPQ is presented. Materials with good thermal stability and good electrical insulating properties were used to form an electrically insulating layer and a physical pixel separator. Each of these layers was patterned using conventional photolithography. The OLED

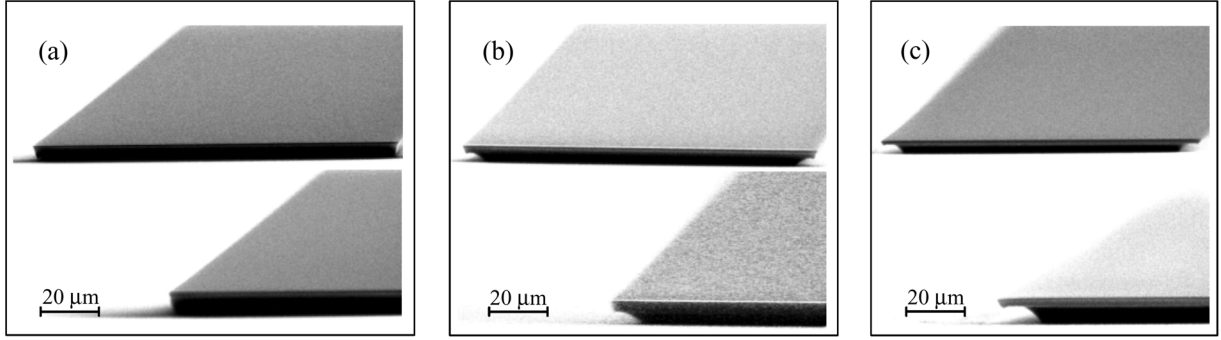


Fig. 2. Scanning electron microscope (SEM) images of a separator layer test pattern for an exposure dose of; (a) 150 mJ/cm<sup>2</sup>; (b) 100 mJ/cm<sup>2</sup>; and (c) 50 mJ/cm<sup>2</sup>.

pixels were fabricated from small molecules deposited from the vapor phase. Instead of PVK, a small-molecule hole-transport material with a high ionization potential was combined with B2PPQ to avoid exciplex formation and to allow for efficient patterning by shadow masking using separators. A current-programming driving circuit was designed and used to address the pixels of the display.

## II. EXPERIMENTAL RESULTS

### A. $M \times N$ OLED Array Fabrication

Early reports of OLED displays showed problems like high leakage current, pixel shrinkage, pixel-to-pixel crosstalk, and nonuniform emission due to edge-field effects between the anode and the metal cathode [5], [6]. Some of these issues have recently been addressed in the literature. It has been shown that separator layers between rows help to prevent pixel-to-pixel crosstalk [7]–[9]. A separator layer with an undercut at the edge can also be used as an integrated shadow mask by ensuring that the vapor-deposited metal cathode is discontinuous between rows [10]. Furthermore, pixel shrinkage and edge-field effects at the anode can be prevented by using an insulator layer that covers the edges of the patterned anode [11]. Both the insulator and the separator layer have to exhibit good electrical insulating properties and should be processable from solution to simplify the fabrication process.

Therefore, three major steps are necessary to fabricate an  $M \times N$  array substrate: patterning of the anode, fabrication of the insulating layer, and deposition of the separator layer. Indium–tin–oxide (ITO) coated-glass substrates with sheet resistance of 20  $\Omega/\square$  (Colorado Concept Coatings, LLC) were used as substrate and as anode for the OLED display. Anode columns and cathode contact pads were defined by patterning the ITO on the glass substrate using the following ITO etching process: after pre-baking of Microposit S1813 positive-type photoresist for 2 min at 100 °C on a hot plate, the film was exposed to UV light through a photo-mask, and then developed by dissolving the previously exposed regions in a Microposit 354 developer. The now exposed ITO was etched using a 5:5:1 mixture of hydrochloric acid (HCl), de-ionized water, and nitric acid (HNO<sub>3</sub>) at a temperature of 45 °C. After etching, the resist was stripped away using acetone, followed by rinsing with de-ionized water.

In the second step, an insulating layer was fabricated. Since an additional layer (separator) had to be patterned subsequently on

top of the insulating layer, we used a heat-resistant PWDC-1000 polyimide (Toray industries, Inc.) with good thermal and chemical resistance to support the second photolithography process. Processing of the insulating layer included the following steps: the positive-type photosensitive polyimide film was pre-baked for 2 min at 120 °C on a hot plate and exposed to UV-light with an energy dose of 200 mJ/cm<sup>2</sup>; the light-exposed regions were then dissolved in a 2.38 % TMAH developer solution for 60 s, and the substrate was rinsed with de-ionized water; and the resulting polyimide pattern was cured for 15 min at 220 °C on a hot plate.

Finally, a separator layer with a well-defined undercut shape was fabricated. To form this separator layer, NR5-8000 negative-type photoresist was first pre-baked for 10 min at 120 °C in a clean oven, followed by UV exposure of 50–100 mJ/cm<sup>2</sup>, and by post-baking of the photoresist for 5 min at 110 °C in the oven. Finally, the film was developed by dissolving the previously unexposed regions in RD6 developer for 60 s. The quality of the undercut was dependent on the energy dose of the UV exposure. Fig. 2 shows three scanning electron microscopy (SEM) pictures of the cross section of the separator layer after UV exposure with different energy doses. At short exposure times [see Fig. 2(c)], the edges of the exposed areas cannot crosslink completely, and the desired undercut shape is observed.

The results of all three processing steps combined is shown in Fig. 3 where part of a finished 11  $\times$  7 pixel substrate with pixel areas of 800  $\mu\text{m} \times$  1000  $\mu\text{m}$  is shown. Film thicknesses of 3  $\mu\text{m}$  and 8  $\mu\text{m}$  were measured for the insulation and the separator layer, respectively.

### B. OLED Structure

In an initial experiment, devices with the well-known small hole-transport molecule  $N,N'$ -bis(*m*-tolyl)- $N,N'$ -diphenyl-1,1'-biphenyl-4,4'-diamine (TPD, Fig. 1) and with B2PPQ as the electron-transport material showed green electroluminescence, which we attribute to exciplex formation. Exciplex emission is dependent on the energy difference between the ionization potential of the hole-transport layer and the electron affinity of the electron-transport layer [12]. If exciplex emission occurs, a red-shift compared to the pure emission of B2PPQ is expected. Therefore, to achieve blue OLEDs, a hole-transport material with higher ionization potential than that of TPD needs to be used.

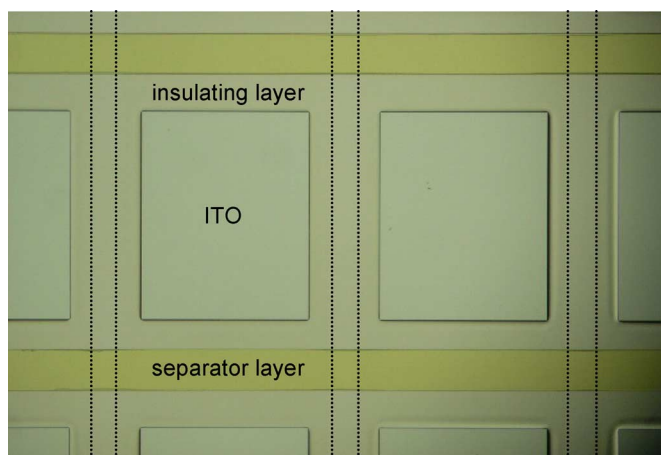


Fig. 3. Microphotography of insulating and separator layers on a patterned ITO substrate for an  $M \times N$  pixel OLED display. The edges of the ITO columns are outlined with dotted lines for better visibility.

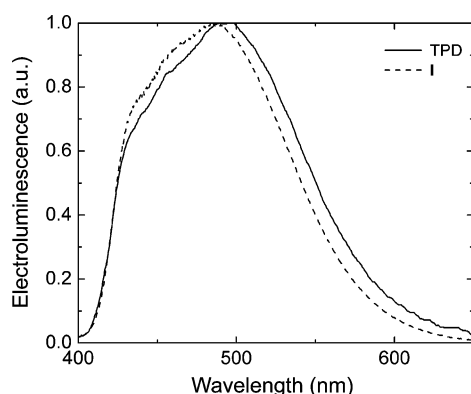


Fig. 4. Normalized electroluminescence spectra of OLED devices with two different hole-transport materials (HTM: TPD or I) and with device structure ITO/HTM (60 nm)/B2PPQ (60 nm)/LiF (1 nm)/Al (200 nm).

TABLE I  
IONIZATION POTENTIALS ( $I_p$ ) OF THE TWO HOLE-TRANSPORT MATERIALS (HTM), PEAK WAVELENGTHS AND CIE COORDINATES ACCORDING TO THE 1931 CONVENTION OF THE ELECTROLUMINESCENCE OF OLED DEVICES WITH DEVICE STRUCTURE ITO/HTM (60 nm)/B2PPQ (60 nm)/LiF (1 nm)/Al (200 nm)

Hole-transport material	$I_p$ (eV) <sup>a</sup>	$\lambda_{\text{peak}}$ (nm)	CIE 1931	
			x	y
TPD	5.38	488	0.19	0.30
I	5.56	486	0.17	0.27

<sup>a</sup> obtained from UV-PES measurements on thin films (see [13]).

We have reported earlier on TPD derivatives in which the ionization potential could be increased by the introduction of electron-withdrawing substituents on the biphenyl amine moiety [13], [14]. Therefore, to avoid the exciplex formation, we chose a fluorinated TPD-derivative (**I**, Fig. 1) as the hole-transport material. Although the ionization potential of this TPD-derivative is only slightly higher than in TPD, a blue-shift of the electroluminescence spectrum of the OLED is clearly visible (Fig. 4). The devices show a light blue emission with CIE 1931 coordinates of  $x = 0.17$ ,  $y = 0.27$  (Table I).

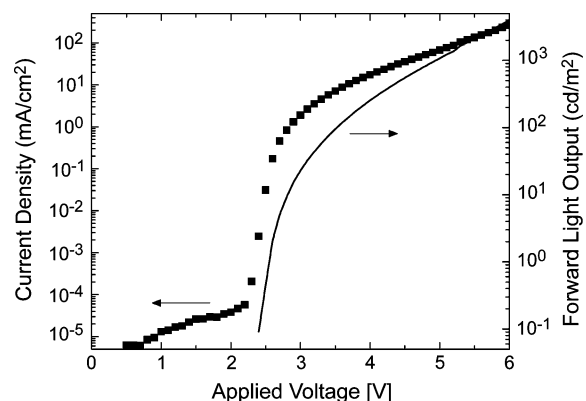


Fig. 5. Current density and luminance versus applied voltage for a blue OLED with device structure ITO/I (60 nm)/B2PPQ (60 nm)/LiF (1 nm)/Al (200 nm).

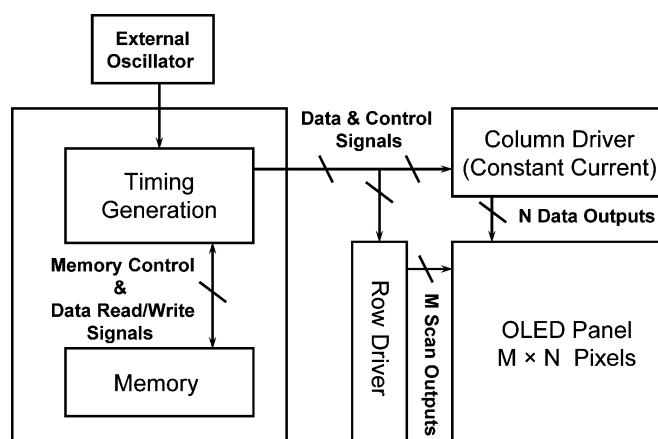


Fig. 6. Schematic of the driving circuitry for an  $M \times N$  pixel OLED display (modified from [17]).

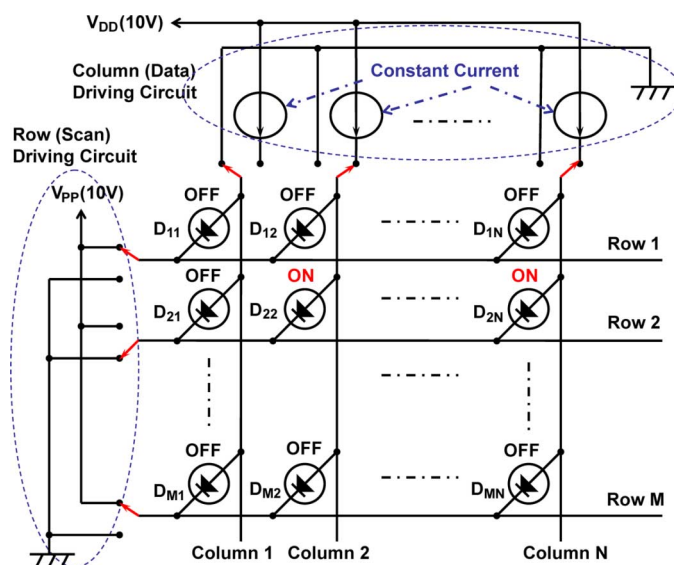


Fig. 7. Schematic of the passive matrix addressing for an  $M \times N$  pixel OLED display.

Current characteristics and luminance as a function of voltage for the blue devices with the hole-transport material **I** and B2PPQ as the electron-transport material are shown in Fig. 5. The devices exhibit an external quantum efficiency of

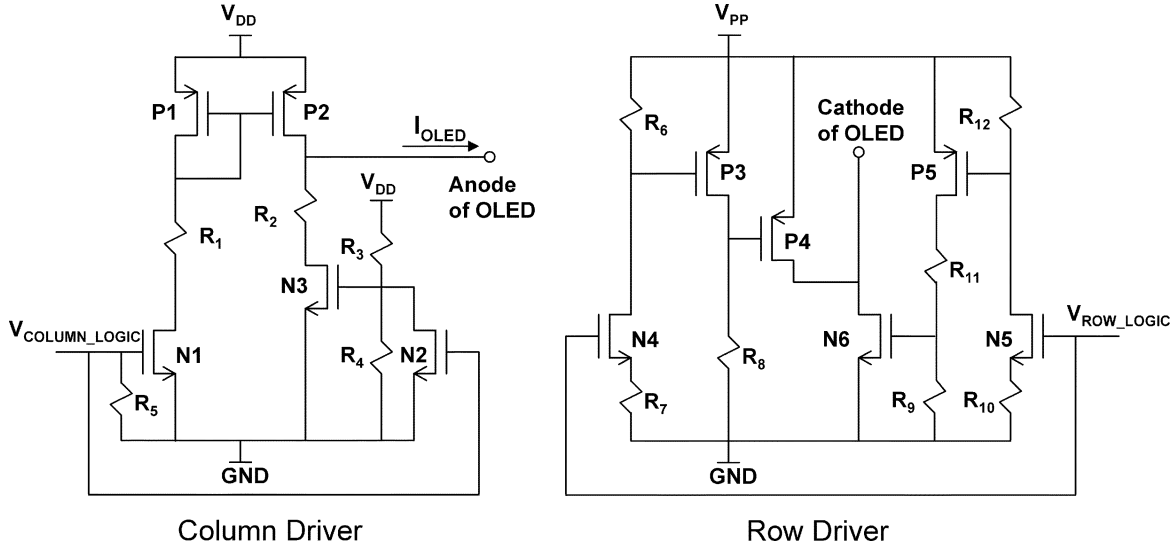


Fig. 8. Column (left) and row (right) driving circuits.

0.7% at 100  $\text{cd/m}^2$ . This decrease in efficiency compared to the OLED previously reported in the literature [4] can be explained by the lower ionization potential of **I** compared to PVK. It has been shown in previous reports that the efficiency of OLEDs increases with increasing ionization potential of the hole-transport material [15], [16]. Therefore, for deep blue light emission and high efficiencies, a small-molecule hole-transport material with an ionization potential comparable to PVK is needed.

**OLED Fabrication:** First, a 40-nm-thick film of the hole-transport material was deposited on the  $M \times N$  pixel substrates using physical vapor deposition. Subsequently, a 40-nm thick film of B2PPQ, previously purified using gradient-zone sublimation, was deposited as electron-transport and emissive layer. Both organic materials were deposited at a rate of 1  $\text{\AA/s}$  and at a pressure below  $1 \times 10^{-7}$  torr. Finally, a 1-nm-thick layer of lithium fluoride (LiF) was deposited as an electron injection layer, followed by a 200-nm-thick Aluminum cathode. LiF and Aluminum were deposited at a rate of 0.1  $\text{\AA/s}$  and 2  $\text{\AA/s}$ , respectively, and at a pressure below  $1 \times 10^{-6}$  torr. All vacuum depositions were performed through shadow masks to protect the contact pads. The testing was done immediately after the deposition of the metal cathode in inert atmosphere without exposing the devices to air.

### C. Drive Electronics Circuit Board

Fig. 6 shows the diagram of the circuitry needed to drive the  $M \times N$  pixel OLED [17] with a detailed view of the passive matrix addressing scheme in Fig. 7. OLEDs are current-driven devices and a current-programming driving circuit is therefore required to address the individual pixels of the display. A current-programming driving circuit provides every pixel with the same current and hence achieves the same brightness for each pixel independently of the voltage drop caused by the sheet resistance along column and row signal lines. To enter the data on the display, the rows are scanned with a duty cycle of  $1/M$ , where the active row is switched to the ground potential while all other rows are held at a high potential to keep the non-selected pixels turned off and avoid crosstalk [18]. An EPLD pro-

grammable IC from the Altera corporation was used as timing chip and was programmed to run at the required frequency. To turn a pixel in a row into the ON state, a constant current is provided to the pixel by the column driving circuit. Columns with pixels in OFF states are grounded.

The detailed column and row driving circuits are shown in Fig. 8 where N, P, and R stands for n-type transistors, p-type transistors and resistors, respectively. Driving circuits for passive matrix displays generally vary in their design and several circuit designs can be used to fulfill the requirements as explained above. The operation of the driving circuits that are used here is explained in the following two paragraphs.

The column driver circuit is based on a current mirror for a constant current supply (N1, P1, and P2) [19] while N2 and N3 are responsible for grounding the column when a pixel is in the OFF state. In detail, the circuit works as follows: if the input voltage  $V_{\text{COLUMN\_LOGIC}}$  goes high (3.3 V), N1 turns on, and a current flows through P1. A matching current also runs through P2. Simultaneously, the input signal is inverted at N2, which causes N3 to be turned off. The current flowing through P2 is therefore only supplied to the OLED pixel and is equal to  $I_{\text{OLED}} = (V_{\text{DD}} - V_{\text{TP}})/R_1$  where  $V_{\text{DD}}$  is the voltage of the power supply (10 V) and  $V_{\text{TP}}$  is the threshold voltage of P1. In the OFF state of the column driver, the low input signal causes N1 to turn off: no current flows through P1 and P2. At the same time, the inverted signal from N2 causes N3 to turn on, and the OLED anode is grounded. All resistors are adjusted to values that provide the proper bias point for each transistor.

The row driver, in contrast, is voltage driven and has the function of grounding the cathode of the OLED in the ON state to ensure unrestricted current flow, and a high bias is applied to the row in the OFF state to set the OLED in reverse-bias. A high input signal  $V_{\text{ROW\_LOGIC}}$  (3.3 V) turns on N4 and N5. Since the drain voltage of N4 is too low to turn off P4, P3 is inserted between these two transistors to boost the input voltage of P3 to the voltage of the power supply and, therefore, turn off P4. Simultaneously, the high input signal turns on N6, and the OLED cathode is grounded. N5 and P5 are equal to N4 and P3 and are

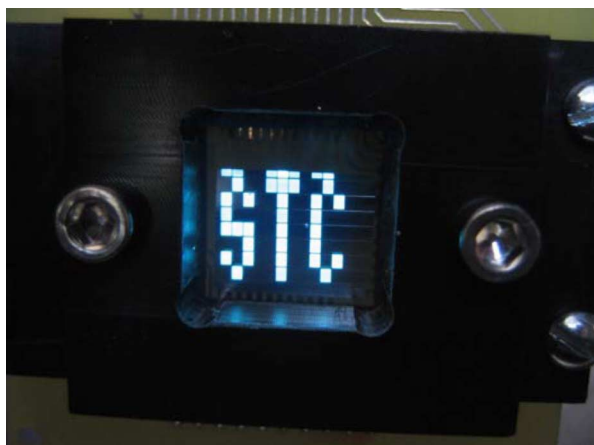


Fig. 9. Photograph of the blue  $11 \times 7$  pixel OLED display.

inserted into the circuit to ensure similar signal delays on P4 and N6. In the OFF state of the row driver, the low input signal turns off N4 and N5 and, therefore, also P3 and P5. The low voltage at the input of P4 and N6 then turns off N6, but turns on P4: a high bias is applied to the cathode of the OLED.

#### D. OLED Display

In a  $7 \times 11$  pixel OLED matrix with a refreshing frequency of 60 Hz, every line is active for 2 ms. The constant current sources were tuned to supply every pixel with an average constant current of  $80 \mu\text{A}$  to achieve a brightness of approximately  $100 \text{ cd/m}^2$ . The final blue  $7 \times 11$  pixel organic light-emitting display is shown in Fig. 9. Due to a slight misalignment of the aluminum cathode, some light emission can be observed in the first row on top of the display.

### III. CONCLUSION

Using chemically and thermally stable materials for an insulation layer and a physical separator, a substrate for a  $7 \times 11$  pixel display was fabricated. The evaporation of a hole-transport material with high ionization potential and the thermally stable and efficient blue fluorescent material B2PPQ with a cathode yielded OLEDs with blue emission and an external quantum efficiency of 0.7% at  $100 \text{ cd/m}^2$ . A constant current driving circuit was used to display letters.

### REFERENCES

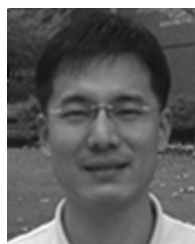
- [1] L. S. Hung and C. H. Chen, "Recent progress of molecular organic electroluminescent materials and devices," *Mater. Sci. Eng.: R: Reps.*, vol. 39, pp. 143–222, 2002.
- [2] W. Shih-Wen, L. Meng-Ting, and C. H. Chen, "Recent development of blue fluorescent OLED materials and devices," *J. Display Technol.*, vol. 1, no. 1, pp. 90–99, Sep. 2005.
- [3] X. H. Yang, D. C. Muller, D. Neher, and K. Meerholz, "Highly efficient polymeric electrophosphorescent diodes," *Adv. Mater.*, vol. 18, pp. 948–954, 2006.
- [4] C. J. Tonzola, A. P. Kulkarni, A. P. Gifford, W. Kaminsky, and S. A. Jenekhe, "Blue-light-emitting oligoquinolines: Synthesis, properties, and high-efficiency blue-light-emitting diodes," *Adv. Funct. Mater.*, vol. 17, pp. 863–874, 2007.
- [5] Y. H. Tak, C. N. Kim, M. S. Kim, K. B. Kim, M. H. Lee, and S. T. Kim, "Novel patterning method using Nd : YAG and Nd : YVO<sub>4</sub> lasers for organic light emitting diodes," *Synth. Metals*, vol. 138, pp. 497–500, 2003.

- [6] D. Braun, J. Rowe, and G. Yu, "Crosstalk and image uniformity in passive matrix polymer LED displays," *Synth. Metals*, vol. 102, pp. 920–921, 1999.
- [7] K. Nagayama, T. Yahagi, H. Nakada, T. Tohma, T. Watanabe, K. Yoshida, and S. Miyaguchi, "Micropatterning method for the cathode of the organic electroluminescent device," *Jpn. J. Appl. Phys. Pt. 2—Lett.*, vol. 36, pp. L1555–L1557, 1997.
- [8] C. Hosokawa, M. Eida, M. Matsuura, K. Fukuoka, H. Nakamura, and T. Kusumoto, "Organic multi-color electroluminescence display with fine pixels," *Synth. Metals*, vol. 91, pp. 3–7, 1997.
- [9] C. Py, M. D'Iorio, Y. Tao, J. Stapledon, and P. Marshall, "A passive matrix addressed organic electroluminescent display using a stack of insulators as row separators," *Synth. Metals*, vol. 113, pp. 155–159, 2000.
- [10] Z. H. Huang, G. J. Qi, X. T. Zeng, and W. M. Su, "A method for undercut formation of integrated shadow mask used in passive matrix displays," *Thin Solid Films*, vol. 503, pp. 246–249, 2006.
- [11] R. Okuda, K. Miyoshi, N. Arai, and M. Tomikawa, "Polyimide coatings for OLED applications," *J. Photopolymer Sci. Technol.*, vol. 17, pp. 207–213, 2004.
- [12] A. C. Morteani, A. S. Dhoot, J. S. Kim, C. Silva, N. C. Greenham, C. Murphy, E. Moons, S. Cina, J. H. Burroughes, and R. H. Friend, "Barrier-free electron-hole capture in polymer blend heterojunction light-emitting diodes," *Adv. Mater.*, vol. 15, pp. 1708–1712, 2003.
- [13] J. D. Anderson, E. M. McDonald, P. A. Lee, M. L. Anderson, E. L. Ritchie, H. K. Hall, T. Hopkins, E. Mash, J. Wang, A. Padias, S. Thayumanavan, S. Barlow, S. Marder, G. Jabbour, S. Shaheen, B. Kippelen, N. Peyghambarian, R. Wightman, and N. Armstrong, "Electrochemistry and electrogenerated chemiluminescence processes of the components of aluminum quinolate/triarylamine, and related organic light-emitting diodes," *J. Amer. Chem. Soc.*, vol. 120, pp. 9646–9655, 1998.
- [14] S. Thayumanavan, S. Barlow, and S. R. Marder, "Synthesis of unsymmetrical triarylamines for photonic applications via one-pot palladium-catalyzed aminations," *Chem. Mater.*, vol. 9, pp. 3231–3235, 1997.
- [15] C. Giebeler, H. Antoniadis, D. D. C. Bradley, and Y. Shirota, "Influence of the hole transport layer on the performance of organic light-emitting diodes," *J. Appl. Phys.*, vol. 85, pp. 608–615, 1999.
- [16] A. Haldi, B. Domercq, R. D. Hrehla, J. Y. Cho, S. R. Marder, and B. Kippelen, "Highly efficient green phosphorescent organic light-emitting diodes with simplified device geometry," *Appl. Phys. Lett.*, vol. 92, p. 253502, 2008.
- [17] H. S. Kim, "Device and method for controlling luminance of flat display," U.S. Patent 6661 428 B1, Dec. 9, 2003.
- [18] Y. Kijima, N. Asai, N. Kishii, and S. I. Tamura, "RGB luminescence from passive-matrix organic LED'S," *IEEE Trans. Electron Devices*, vol. 44, no. 8, pp. 1222–1228, Aug. 1997.
- [19] H. S. Kim and Y. S. Na, "Current control circuit for display device of passive matrix type," U.S. Patent 6633 136 B2, Oct. 14, 2003.



**Andreas Haldi** received the diploma in interdisciplinary science with a focus on optics and solid-state physics from ETH Zurich, Zurich, Switzerland, in 2003, and is currently working towards the Ph.D. degree in electrical engineering at the Georgia Institute of Technology, Atlanta.

His research is focused on organic light-emitting diodes.



**Jung B. Kim** received the B.S. degree in electrical engineering from Kyungpook National University, and the M.S. degrees from Seoul National University, Korea, in 1993 and 1997, respectively, both in electrical engineering. He is currently working toward the Ph.D. degree in electrical and computer engineering at the Georgia Institute of Technology, Atlanta, where he is focusing on organic and inorganic TFTs and active matrix OLED displays.

From 1997 to 2002, he was a research engineer in the OLED group at the LG Institute of Technology,

Korea.



**Benoit Domercq** was born in France. He studied at the Ecole Normale Supérieure, Lyon, France, and received the M.S. degree in physical chemistry from Ecole Polytechnique, Palaiseau, France, in 1995, and the Ph.D. degree in material chemistry from the University of Nantes, Nantes, France, in 1999.

From 1999 to 2003, he was a research scientist at the Optical Sciences Center at the University of Arizona focusing on the development of organic materials for light-emitting, light-harvesting and charge transport applications. He has coauthored over 40 refereed publications in the area of organic optoelectronic materials and devices. Since 2003, he has been with the research faculty of the newly created Center for Organic Photonics and Electronics (COPE), Georgia Institute of Technology.

**Abhishek P. Kulkarni**, photograph and biography not available at the time of publication.

**Stephen Barlow**, photograph and biography not available at the time of publication.

**Angela P. Gifford**, photograph and biography not available at the time of publication.

**Samson A. Jenekhe**, photograph and biography not available at the time of publication.

**Seth R. Marder**, photograph and biography not available at the time of publication.



**Bernard Kippelen** (M'05–SM'05) received the Ph.D. degree in solid-state physics from the University Louis Pasteur, Strasbourg, France, in 1990.

He was Chargé de Recherches at the CNRS, France. In 1994 he joined the Optical Sciences Center, The University of Arizona, where he became an Assistant Professor in 1998, and Associate Professor in 2001. Since 2003, he has been with the Georgia Institute of Technology, Atlanta, as Professor of Electrical and Computer Engineering.

Prof. Kippelen is a Fellow of the Optical Society of America and a Fellow of SPIE.